

# Near Future Weather Data for Building Energy Simulation in Summer/Winter Seasons in Tokyo Developed by Dynamical Downscaling Method

Yusuke ARIMA<sup>1</sup>, Ryozo OOKA<sup>2</sup>, Hideki KIKUMOTO<sup>3</sup>, Toru Yamanaka<sup>4</sup>

Yusuke  
ARIMA

<sup>1</sup> Graduate School of Engineering, The University of Tokyo, 4-6-1 Komaba, Meguro-ku, Tokyo 153-8505, Japan,  
arima-y@iis.u-tokyo.ac.jp

<sup>2</sup> Institute of Industrial Science, The University of Tokyo, 4-6-1 Komaba, Meguro-ku, Tokyo 153-8505, Japan,  
ooka@iis.u-tokyo.ac.jp

<sup>3</sup> Institute of Industrial Science, The University of Tokyo, 4-6-1 Komaba, Meguro-ku, Tokyo 153-8505, Japan,  
kkmt@iis.u-tokyo.ac.jp

<sup>4</sup> Kajima Technical Research Institute, Kajima Corporation, 2-19-1 Tobitakyu, Chofu, Tokyo 182-0036, Japan,  
t-yamanaka@kajima.com

## 1. Introduction

Climate change phenomena, such as global warming and urban heat island effects, is progressing [1]. Mitigation and adaptation are the two approaches for coping with global warming. For mitigation in the construction sector, buildings are required to improve the energy efficiency to reduce CO<sub>2</sub> emissions, which is the main cause of global warming. Further, the adaptation of building designs to climate change is required to continue developing comfortable indoor environments in the future. During the design process, energy simulations are often used to evaluate the indoor thermal environment and energy consumption of buildings [2]. In these simulations, the regional weather data known as typical weather data or design weather data, usually based on current or past weather events, are commonly used [3]. However, most buildings have existed for several decades, during which the climate conditions have gradually changed. Therefore, the development of weather data for the future and the assessment of the impact of climate change on buildings have become very important for both mitigation and adaptation purposes [4, 5].

We have attempted to construct the near-future weather data for architectural design using numerical meteorological models. Climate data projected by Global Climate Models (GCMs) are available for future weather data. Although GCMs can predict long-term global warming, they cannot illustrate the details of the local phenomena due to their coarse grid resolution (~100 km). Therefore, we input the GCM data to a Regional Climate Model (RCM) as the initial and boundary conditions. Then, the data is physically downscaled with the RCM. This process is known as dynamical downscaling [6, 7]. The RCM uses nested regional climate modeling and can provide high-resolution (~1 km) local climate data. Weather predictions made through this method is expected to represent global climate change and local phenomena such as urban heat islands [8, 9].

Similar previous studies on producing future weather data and assessing the effect of climate change on building energy consumption have been conducted. For example, Hacker developed a method for producing future weather data, and this method is known as the morphing method [10]. Crawley also produced future weather data from existing typical weather data by using the morphing method and calculated the impact of climate change on a small office building [11]. In the morphing method, future weather data is produced by morphing current observation data using the difference between current and future weather conditions. Therefore, daily weather disturbance of the future weather data obtained through the morphing method is based on that of current observation. Weather disturbance is an important component of weather data for building energy simulations, particularly for estimating the peak demand. However, future weather data obtained through the morphing method could not represent disturbance predicted by the GCM. On the other hand, the daily disturbance predicted by the dynamical downscaling method is based on future climatic conditions predicted by the GCM. This is one of the advantages of our method over the morphing method.

In this study, we conducted climate simulations in January and August for the present and future. First, we dynamically downscaled the current climate data projected by MIROC4h for the current period (2001-2010) to confirm the reproducibility of the current climate conditions. Next, we produced future weather data by downscaling the MIROC4h for the near-future period (2026-2035) and confirmed the climate change reproducibility of the weather data. The output from weather and climate models includes statistical error or bias, which becomes problematic when the output is directly used for the building energy simulations. Thus, we corrected the bias of the weather data using the statistical values of observations and WRF results, and constructed a prototype of future weather data for building energy simulations. We conducted the building energy simulations using these prototypes to assess the impact of climate change on building energy loads during summer and winter.

## 2. Dynamical Downscaling

### 2.1 Analysis Conditions

We employed the Model for Interdisciplinary Research on Climate version 4 (MIROC4h) as the GCM. MIROC4h was developed by the Center for Climate System Research, the National Institute for Environmental Studies (NIES), and the Frontier Research Center for Global Change. MIROC4h reproduces global warming at a horizontal scale of approximately 60 km [12, 13]. For the current (2001–2010) simulations, we used the output of MIROC4h projected from 1981. For the near-future (2026–2035) simulations, we used the output of MIROC4h projected from 2006. Future climate conditions were projected by the GCM, assuming the concentrations of warming-effect gases, such as CO<sub>2</sub>, will change in the future; these projected conditions are known as scenarios. The scenario adopted by MIROC4h simulations is RCP4.5 [14, 15] defined by the Intergovernmental Panel on Climate Change (IPCC) [1]. Based on the warming intensity, the RCPs have four representative pathways, RCP8.5, RCP6.0, RCP4.5 and RCP2.6, mainly because of the differences in the greenhouse gas concentrations, and RCP4.5 is the third strongest scenario. There were not many differences in radiative forcing among RCPs for the near future, which was the focus of this study. In the projection by MIROC4h based on RCP4.5, the surface temperature (at 2 m) in Tokyo increased by 1.05°C from the current to the near future, and surface absolute humidity increased by 0.00126 kg/kg.

We used the Weather Research and Forecasting (WRF) model, version 3.4, as the RCM [16]. The WRF model was mainly developed by the National Center for Atmospheric Research and is commonly used for local climate studies. We used U.S. Geological Survey (USGS) 24-category land use data for domain 1, 2, 3 and National Land Numerical Information for domain 4, which provides a more realistic data for the urban areas. Fig.1 shows the nesting regions of the WRF. The target areas in this study are the Kanto region in Japan and particularly Tokyo (in this study, Tokyo means Otemachi, which is located center of the Tokyo) along with its surrounding area. We used four levels of nested regional climate modeling, in which the first and fourth levels have horizontal spatial resolutions of 54 km and 2 km, respectively. We used the Noah land surface model (Noah LSM) as a land physics scheme. The Noah LSM [17] requires soil temperature and humidity, which are not included in MIROC4h daily output or shorter. Thus, we also complementally used the National Centers for Environmental Prediction (NCEP) Final Operational Global Analysis (FNL) data [18] for soil temperature and humidity for the simulations by using MIROC4h. The weather component list of MIROC4h data are presented in Table 1 and the applied physics scheme is listed in Table 2. Analysis is conducted during January 1–31 and August 1–31 in each year. Two weeks spin up run was carried out in each simulation. Please refer to the previous report for more detailed analysis conditions [19].

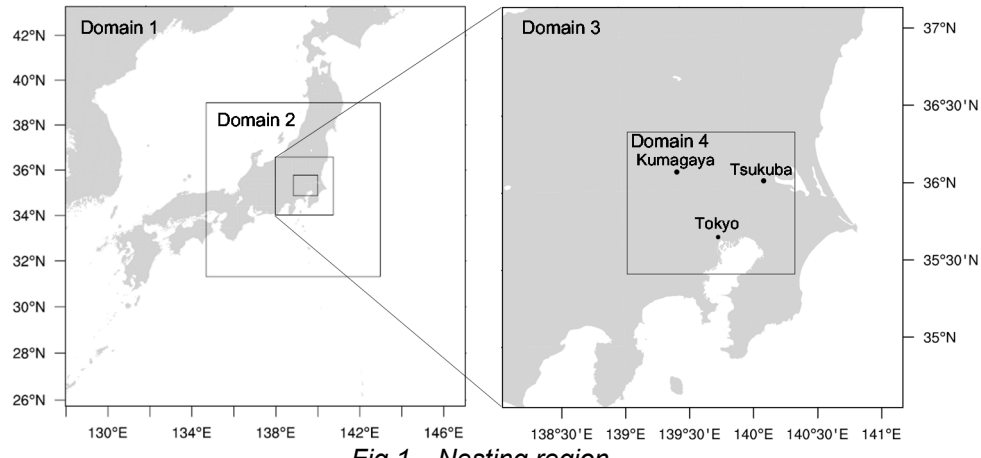


*Fig.1 Nesting region*

*Table1 Weather components used as initial and boundary conditions in WRF simulation*

Longitude, Latitude	0.5625°
Time	6 h
Weather elements at 17 layers	Temperature, specific humidity, wind velocity, geopotential height,
Surface	Surface temperature, sea surface pressure, sea surface temperature

※17 layers (1000, 950, 900, 850, 700, 500, 400, 300, 250, 200, 150, 100, 70, 50, 30, 20, 10 [hPa])

*Table2 Physics scheme of WRF*

Cumulus parameterization	Domains 1 & 2: Kain-Fritsch; Domains 3 & 4: none
Microphysics	WRF single-moment six-class scheme
Planetary boundary layer	Yonsei University scheme
Longwave radiation	RRTM scheme
Shortwave radiation	Dudhia scheme
Land surface	Noah land surface model (Noah LSM)
Sea surface update	On (6-h interval)
Nudging	Off

## 2.2 Reproducibility of Current Climate Conditions

We compared the statistical value of downscaled current (2001–2010) output of MIROC4h with that of observations (OBS) to confirm that the current downscaled MIROC4h can reproduce current climate conditions presented by OBS. We named the simulation for current climate conditions as Case 1 and that for future climate conditions as Case 2. Table 3 shows the monthly average of the ten-year mean of each weather component for January and August. The temperature differences (at 2m) between Case 1 and OBS were 0.54°C and 1.84°C in August and January, respectively. The monthly average water vapor pressure (at 2 m) in Case 1 was 1.19 hPa lower than the OBS in August and 0.37 hPa higher than the OBS in January. Regarding radiation, the results of Case 1 were overestimated, compared with OBS in both January and August. If the spatial representativeness of the observation data was not taken into account, the difference between Case1 and OBS was due to statistical errors, or bias of climate/weather model.

*Table 3 Average of each weather component in Tokyo in August and January  
(Horizontal solar radiation and atmospheric radiation are monthly mean sun integrated value)*

	Temperature [°C]	Water vapor pressure [hPa]	Horizontal solar radiation [MJ/m <sup>2</sup> ]	Atmospheric radiation [MJ/m <sup>2</sup> ]	Wind velocity [m/s]
OBS (Aug)	27.5	25.1	15.5	-	3.13
CASE1(Aug)	28.1 (0.54)	23.9 (-1.19)	19.5 (3.96)	35.8	3.72 (0.60)
CASE2 (Aug)	29.2 (+1.11)	25.7 (+1.81)	19.5 (-0.05)	36.6 (+0.94)	3.76 (+0.03)
OBS (Jan)	6.26	4.33	9.31	-	3.28
CASE1 (Jan)	8.10 (1.84)	4.69 (0.37)	10.6 (1.32)	22.4	3.90 (0.62)
CASE2 (Jan)	8.70 (+0.60)	4.89 (+0.20)	10.6 (-0.02)	22.6 (+0.17)	3.79 (-0.11)

Next, we confirmed the reproducibility of regional characteristics obtained by dynamical downscaling. Fig.2 shows the monthly averaged temperature at 2m daily change over ten years in each three cities, Tokyo (35.9°N, 139.76°E), Tsukuba (36.06°N, 140.12°E), and Kumagaya (36.15°N, 139.38°E). Considering both the results of Case 1 and OBS, the largest amount of diurnal temperature range was in Kumagaya, followed by Tsukuba and Tokyo. The reproducibility of the regional characteristics by dynamical downscaling was confirmed.

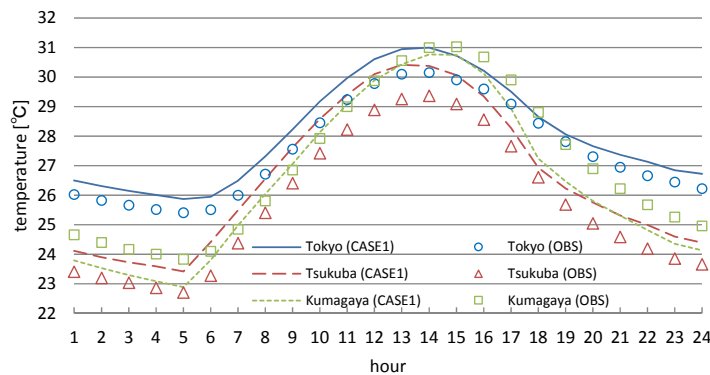


*Fig.2 Ten years averaged daily temperature change at Tokyo, Tsukuba, and Kumagaya for current climate conditions (2001-2010)*

## 2.3 Changes in Weather Components between the Present and Future

The climate information projected by MIROC4h takes into consideration climate change phenomena such as global warming. Therefore, the weather data obtained by the downscaling of MIROC4h data is also expected to reproduce climate change. We dynamically downscaled future (2026–2035) weather data projected by MIROC4h (Case 2) and compared the monthly average of the ten-year mean for Case 1 and Case 2 in Table 3. The monthly average temperature increases by 1.11°C and 0.60°C August and January, respectively. The monthly average water vapor pressure increases by 1.81hPa in August and 0.20hPa in January. Regarding both the temperature and water vapor pressure, the difference between Case 1 and Case 2 in August is higher than in January. With regard to horizontal atmospheric radiation, monthly mean sun integrated value increases by 0.94MJ/m<sup>2</sup> in August and 0.17MJ/m<sup>2</sup> in January. Solar radiation and wind velocity do not change significantly between Case 1 and Case 2.

## 3. Constructing Prototype of Future Weather Data

As described in section 2.2, the outputs of the weather and climate models have unique bias for each model, including the coarse resolutions and inaccuracy of the parameterization. Therefore, bias correction is required when directly using the output of weather and climate models as practicable weather data for building energy simulations. In this study, we corrected the biases of temperature, humidity, and radiation projected by the GCM and RCM. The

one-hour interval temporal weather data  $X_c$  of temperature and humidity was corrected using equation (1), which uses the average  $\bar{X}_c$  and the standard deviation  $\sigma_c$  of WRF results, and the average  $\bar{X}_{obs}$  and standard deviation  $\sigma_{obs}$  of OBS. In equation (2) for Case 2, the climate change term  $(\bar{X}_f - \bar{X}_c)$  was added to equation (1). With regard to radiation, we used equations (3) and (4), which use the ratio  $\bar{X}_{obs}/\bar{X}_c$  of the average of Case1 to that of OBS.

$$X_{c,modi} = \bar{X}_{obs} + \frac{\sigma_{obs}}{\sigma_c} (X_c - \bar{X}_c) \quad (1)$$

$$X_{f,modi} = \bar{X}_{obs} + (\bar{X}_f - \bar{X}_c) + \frac{\sigma_{obs}}{\sigma_c} (X_f - \bar{X}_f) \quad (2)$$

$$X_{c,modi} = \frac{\bar{X}_{obs}}{\bar{X}_c} X_c \quad (3)$$

$$X_{f,modi} = \frac{\bar{X}_{obs}}{\bar{X}_c} X_f \quad (4)$$

## 4. Building Energy Simulation for Near-Future Data

### 4.1 Building Energy Simulation Conditions

We conducted building energy simulations in August and January for the current period (2001-2010) and near-future period (2026-2035). We used the TRAnsient SYstem Simulation Tool (TRNSYS17), which is a dynamic energy simulation software package [20]. The bias-corrected weather data simulated by the WRF (WD) was used as the input weather data. The target was a two-story detached house model IBEC defined as a standard Japanese house for building energy simulation (Fig.3). The thermal property of the house is shown in Table 4. The location was assumed to be Tokyo. The living room and dining kitchen (LDK), bedroom, and two children's rooms required air conditioning, and the schedule of air conditioning is shown in Table 5. The rate of general ventilation was 0.5/h.

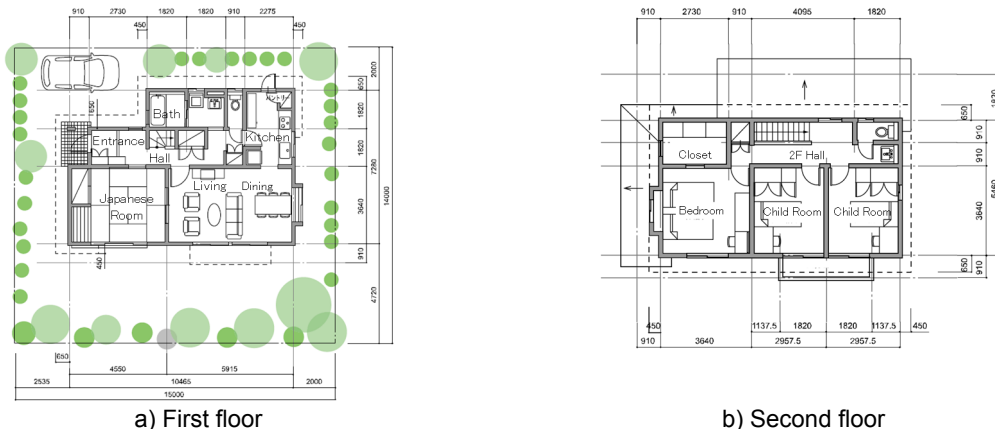


Fig.3 Plans of the model house (the standard house model in Japan) used in the building energy simulation

Table 4 Thermal property of the model house

Component	Heat transmission coefficient [W/m <sup>2</sup> K]	Solar absorptance [-]	Convective heat transfer coefficient [W/m <sup>2</sup> K]
External wall	0.385	0.8	3.05 (indoor), 17.7 (outdoor)
Roof	0.294	0.8	3.05 (indoor), 17.7 (outdoor)
Window	5.72	0.875 (Solar heat gain coefficient)	3.05 (indoor), 17.7 (outdoor)

Table 5 Air conditioning setting  
a) Cooling

ROOM	Preset temperature [°C]/Relative temperature [%]	Schedule of air conditioning
LDK	27 /60	6:00–10:00, 12:00–14:00, 16:00–24:00
BEDROOM	27 (sleep 28) /60	(sleep 23:00–7:00)
CHILD ROOM 1	27 (sleep 28) /60	(sleep 00:00–7:00), 20:00–21:00, 22:00–24:00
CHILD ROOM 1	27 (sleep 28) /60	(sleep 00:00–7:00), 18:00–19:00, 21:00–23:00, (sleep 23:00–24:00)

b) Heating

ROOM	Preset temperature [°C]	Schedule of air conditioning
LDK	20	6:00–10:00, 12:00–14:00, 16:00–24:00
CHILD ROOM 1	20	20:00–21:00, 22:00–24:00
CHILD ROOM 1	20	18:00–19:00, 21:00–23:00

## 4.2 Estimation of the Impact of Climate Change on the Monthly Heat Load

Table 6 shows the monthly heat load in all the rooms in August and January for the ten-year mean. In August, the sensible heat load increases by 13%, latent heat load increases by 19%, and total heat load (sensible and latent heat load) increases by 14% from current (WD\_Aug 2001-2010) to future (WD\_Aug 2026-2035). In January, the sensible heat load decreases by 9% from current (WD\_Jan 2001-2010) to future (WD\_Jan 2026-2035). Climate change has increased the energy demand in summer and has decreased in winter. The sum of the total heat load , both in August and January, increases by 8% from current to future weather data.

**Table 6** Monthly heat load at all rooms in August and January for the ten-year mean  
a) August

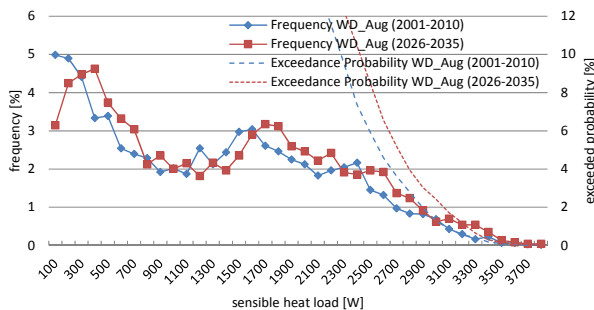
Input weather data	Sensible heat load [MJ/month]	Latent heat load [MJ/month]	Total heat load [MJ/month]
WD_Aug (2001-2010)	$2.55 \times 10^3$	$6.87 \times 10^2$	$3.23 \times 10^3$
WD_Aug (2026-2035)	$2.88 \times 10^3$ (113%)	$8.18 \times 10^2$ (119%)	$3.70 \times 10^3$ (114%)
b) January			
Input weather data	Sensible heat load [MJ/month]		
WD_Jan (2001-2010)	$1.25 \times 10^3$		
WD_Jan (2026-2035)	$1.14 \times 10^3$ (91%)		

## 4.3 Estimation of the Impact of Climate Change on Maximum Heat Load

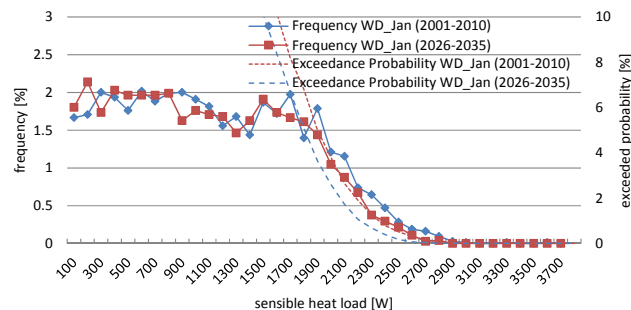
We assessed the impact of climate change on the maximum heat load. The maximum heat load is defined as the topmost 0.5% among the heat loads for 10 years (7440hours). Table 7 shows the maximum heat load of the present and future, and Fig.4 shows the frequency of sensible heat load and exceedance probability. In August, the maximum sensible heat load increases by 2%, maximum latent heat load increases by 9% and maximum total heat increases 2% from current to future weather data. In January, the maximum sensible heat load decreases by 6% from current to future weather data. The impact of climate change on the maximum heat load (2%) will be smaller than that on the mean monthly heat load (14%).

**Table 7** Maximum heat load in August and January for 10 years  
a) Summer

Input weather data	Sensible heat load [kW]	Latent heat load [kW]	Total heat load [kW]
WD_Aug (2001-2010)	3.35	1.12	3.79
WD_Aug (2026-2035)	3.42 (102%)	1.24 (109%)	4.14 (102%)
b) Winter			
Input weather data	Sensible heat [kW]		
WD_Jan (2001-2010)	2.61		
WD_Jan (2026-2035)	2.46 (94%)		



a) August



b) January

**Fig.4** Frequency of sensible heat loads for 10 years and exceedance probability at all rooms  
(Solid line and dashed line shows frequency and exceedance probability, respectively)

## Conclusions

In this study, we assessed the impact of climate change on the building energy demand of a two-story detached house in Tokyo using near-future weather data directly by using a dynamically downscaled output from the MIROC4h. Because of global warming, building energy demand increases in summer and decreases in winter. Under such conditions, the sum of the total heat load in August and January increases 8% from current to future simulations. In addition, we assessed the impact of climate change on the maximum heat load. The maximum heat load increases by 2% in August and decreases by 6% in January. The impact on the maximum heat load is smaller than that of the mean monthly heat load. The impact of climate change on maximum heat load, which was assessed in this study, is difficult to assess using the existing future weather data by the morphing method because the daily disturbance of the future weather data is based on current observations.

For future work, by using the ensemble average method on several GCMs output, responsibility should be enhanced and the band of the predictions should be presented. Urban change can be considered at the mesoscale level (a few kilometers) using the dynamical downscaling method, which is one of the merits of our method. However urban change was not considered in this study. If urban growth intensifies, energy consumption for cooling would increase because of the heat island effect. However, accurate estimation of future urban condition is difficult. When attempting to create future weather data considering urban change, we must suggest possible future urban scenarios. This task is a challenge for future studies.

## Acknowledgment

This study represents a part of the research conducted by the working group on the near-future standard weather data using global climate modeling (Project General Manager: Ryozo Ooka) [21]. The authors are very grateful to the WG members (Satoru Iizuka, Akashi Mochida, Akira Kondo, Hideyo Nimiya, Ryuichiro Yoshie, Shinji Yoshida, and Tsubasa Ookaze) and express their gratitude to the Kimoto laboratory of the Atmosphere and Ocean Research Institute, University of Tokyo, which provided the MIROC4h data for the present study. Part of this work was supported by JSPS KAKENHI Grant Number 24226013 "Development of a meteorological information platform with high spatial resolution for the urban environment and disaster reduction" (Project General Manager: Ryozo Ooka).

## References

- [1] Intergovernmental Panel on Climate Change, 2013: Working group I contribution to the IPCC Fifth Assessment Report (AR5), Climate Change2013, The Physical Science Basis.
- [2] Kohri K., Ishino H., 2005: Examination on Expanded AMeDAS Design Weather Data for HVAC Systems, Journal of Asian Architecture and Building Engineering 4(2), pp.541-548.
- [3] Cooperman A., et al, 2010: Using Weather Data for Predictive Control, ASHRAE Journal, pp.130-132.
- [4] Robert, A., Kummert, M., 2012: Designing Net-zero Energy Buildings for the Future Climate, not for the Past, Building and Environment, 55, pp.150-158.
- [5] Jentsch, M. F., Vahaj, A. S., James, P. A.B., 2008: Climate Change Future Proofing of Buildings – Generation and Assessment of Building Simulation Weather Files, Energy and Buildings, 40, pp.2148-2168.
- [6] Dickinson, R.E. et al., 1989:A Regional Climates Model for the Western United States, Kluwer Academic Publishers, Climate Change 15, pp.383-422.
- [7] Giorgi F., Bates T., 1989: The Climatological Skill of a Regional Model over Complex Terrain, Monthly Weather Review, 117, pp.2325-2347.
- [8] Wang, Y. et al., 2004: Regional Climate Modelling, Progress, Challenges, and Prospects, Journal of the Meteorological Society of Japan, 82(6), pp.1599-1628.
- [9] Kikumoto, H. et al., 2015. Study on the Future Weather Data Considering the Global and Local Climate Change for Building Energy Simulation. Sustainable Cities and Society 14, pp. 404-413.
- [10] Belcher, S.E., Hacker, J.N., 2005: Constructing Design Weather Data for Future Climates, Building Services Engineering Research & Technology, 26(1), pp.49-61.
- [11] Crawley, 2008: Estimating the Impacts of Climate Change and Urbanization on Building Energy Performance, Journal of Building Performance Simulation, 1(2), pp.91-115.
- [12] Nozawa, T. et al., 2007: Climate Change Simulations with a Coupled Ocean-atmosphere GCM called the Model for Interdisciplinary Research on Climate: MIROC, CGER's Supercomputer Monograph Report 12 (NIES).
- [13] Sakamoto, T., 2012: MIROC4h-A New High-Resolution Atmosphere-Ocean Coupled General Circulation Model, Journal of the Meteorological Society of Japan, 90(3), pp.325-359.
- [14] Meinshausen, M. et al., 2011: The RCP Greenhouse Gas Concentrations and their Extensions from 1765 to 2300.
- [15] Richard, H. et al., 2010: The Next Generation of Scenarios for Climate Change Research and Assessment, Nature, 463, pp.747-756.
- [16] Skamarock, W.C. et al. 2008: A Description of the Advanced Research WRF Version 3, NCAR Technical Note, NCAR/TN-475+STR
- [17] Chen, F., Dudhia J., 2001: Coupling an Advanced Land-surface/ Hydrology Model with the Penn State/ NCAR MM5 Modeling System. Part I: Model Description and Implementation, Monthly Weather Review, 129, pp.569–585.
- [18] NCAR Data Support Section: CISL Research Data Archive, <http://rda.ucar.edu/datasets/ds083.2/>
- [19] Kikumoto, H., et al. 2014: Study on the Future Weather Data Considering the Global and Local Climate Change for Building Energy Simulation, Sustainable Cities and Society, 14, pp.404-413.
- [20] The University of Wisconsin: The official TRNSYS website, <http://sel.me.wisc.edu/trnsys/index.html>
- [21] Working Group for Future Standard Weather Data using GCM results, Sub-committee on Urban and Climate Adaptation, Research Committee on Global Environment, 2014: The Near Future Weather Data for Building Energy Simulation Using Dynamical Downscaling of Results from Global Climate Model, AJJ Journal of Technology and Design, 20(4), pp.1041-1046.